Avoiding stair-step artifacts in image registration for GOES-R navigation and registration assessment

Thomas J. Grycewicz*[a], Bin Tan[b,d], Peter J Isaacson[a], Frank J. De Luccia[a], John Dellomo[c,d]
[a]The Aerospace Corporation, 2310 E. El Segundo Bl., El Segundo, CA USA 90245-4691, [b]SSAI, 10210 Greenbelt Rd., Suite 600, Lanham, MD USA 20706, [c]GST, 7855 Walker dr., Suite 200, Greenbelt, MD USA 20770, [d]NASA GSFC Terrestrial Information Systems Laboratory,8800 Greenbelt RD., Greenbelt, MD 20771.

ABSTRACT

In developing software for independent verification and validation (IV&V) of the Image Navigation and Registration (INR) capability for the Geostationary Operational Environmental Satellite – R Series (GOES-R) Advanced Baseline Imager (ABI), we have encountered an image registration artifact which limits the accuracy of image offset estimation at the subpixel scale using image correlation. Where the two images to be registered have the same pixel size, subpixel image registration preferentially selects registration values where the image pixel boundaries are close to lined up. Because of the shape of a curve plotting input displacement to estimated offset, we call this a stair-step artifact. When one image is at a higher resolution than the other, the stair-step artifact is minimized by correlating at the higher resolution. For validating ABI image navigation, GOES-R images are correlated with Landsat-based ground truth maps. To create the ground truth map, the Landsat image is first transformed to the perspective seen from the GOES-R satellite, and then is scaled to an appropriate pixel size. Minimizing processing time motivates choosing the map pixels to be the same size as the GOES-R pixels. At this pixel size image processing of the shift estimate is efficient, but the stair-step artifact is present. If the map pixel is very small, stair-step is not a problem, but image correlation is computation-intensive. This paper describes simulation-based selection of the scale for truth maps for registering GOES-R ABI images.

Keywords: GOES-R, image registration, systematic error, stair-step artifact

1. INTRODUCTION

Stair-step[1] is a systematic artifact in sub-pixel level image registration processes which has been seen while testing the Image Navigation and Registration (INR) Performance Assessment Tool Set (IPATS). IPATS is being developed by the GOES-R Flight Project to provide a capability for evaluation of post launch INR performance of the Advanced Baseline Imager (ABI) and the Geostationary Lightning Mapper (GLM).[2] IPATS uses image registration to estimate the sub-pixel offset between an image chip extracted from the Level 1-B GOES product and a second image, which may be a reference image of the ground, a sub-image extracted from the same GOES product or an image taken earlier the same day. To characterize ABI and GLM image navigation (NAV), IPATS will register the satellite images to reference image chips with known ground truth. The ground truth chipset used by IPATS includes the landmarks[3] used by the GOES-R ground system's Product Monitor (PM) as well as many other high contrast local regions on the earth. Frame-to-frame registration (FFR) will register images where successive images have clear, cloud-free see-to-ground view at the same location. A Swath-to-Swath Registration (SSR) process is being developed to characterize how well the image swaths in a whole earth image are aligned. ABI Channel-to-Channel Registration (CCR) is possibly the most challenging characterization since IPATS must register images between different wavebands with inherently different spectral content. This study focuses on image registration, which is common to all of these processes.

The stair-step artifact is a registration error encountered when attempting to interpolate the registration of pixelated images to subpixel accuracy. We became aware of this several years ago when investigating analog optical image correlators[1]. The effect of the artifact is a systematic bias of the image registration towards the nearest shift of an integer number of pixels. Thus, the estimate returned for shifts of less than half a pixel are shortened relative to true shift, while estimates for shifts between a half pixel and a full pixel are lengthened. The effect is typically small, of order a tenth of a pixel. But this error magnitude places it on a scale similar to the INR accuracy requirements for the GOES-R ABI system.[4]

*Thomas.J.Grycewicz@aero.org; phone 1(571)307-3857

Early in the process of building IPATS, we tested the algorithms using simulated GOES-R ABI images built using Landsat images as a basis set. Since Landsat images have a Ground Sample Distance (GSD) of 30 m and the ABI GSD is 500 m at nadir for the highest resolution 0.64 μm band and larger elsewhere, the Landsat images provide a very densely sampled view of the ground from which to build simulated GOES images.

This paper will characterize the stair-step artifact using a scene evaluated with IPATS to assess the impact of the stair-step artifact on algorithms used to assess INR performance of GOES-R. Methods for estimating the effect of stair-step on INR assessments and reducing the amount of stair-step error in INR characterization estimates will be discussed. Stair-step is seen most strongly when the images to be registered are very similar. This paper will focus on single band correlation as seen in ABI simulations of NAV, FFR, and SSR.

This paper will limit correlator discussion to the case of the Normalized Cross-Correlator (NCC), which calculates the Pearson correlation coefficient between two images,[5,6] as implemented in the OpenCV (Open Source Computer Vision) programming function library.[7] Evidence of a stair-step artifact has been seen when the other correlators are used, but will not be discussed in this paper.

This paper is also limited to correlation in a single spectral band. Evidence for the stair-step artifact is seen when correlating between two similar bands, such as blue to red, red to near IR, or between two long-wave IR channels. But in these cases the stair-step effect is mixed noise arising from the difference between the channels. This paper is an introduction to the stair-step effect as seen in the IPATS data and will be limited to the single band case where the stair-step signal is very clear and clean. Single band correlation is used within IPATS for the NAV, FFR, and SSR processes.

1. THE STAIR-STEP ARTIFACT

Figure 1.1-1 shows a portion of a Landsat 8 scene which was used during early development of the IPATS algorithm set. A set of 8 windows were constructed in the region northeast of San Diego, CA. Each 1200x1200 pixel Landsat window was reduced to a 48x48 pixel surrogate GOES window through 25x25 pixel aggregation. Fifty-one sets of these windows were made with single Landsat pixel eastward shifts, for a total shift of two GOES pixels. Two image sets from Landsat8 band 4 (red) were used, from Feb 05, 2014, and Sep 30, 2014.[8]

1.1 Characteristics of the stair-step artifact

The plots in Figure 1 illustrate the stair-step artifact. The center plot shows the shift estimate, and the right plot shows the error determined by subtracting the actual image shift from the estimated image shift. The RMS value of this error is 0.06 pixels.

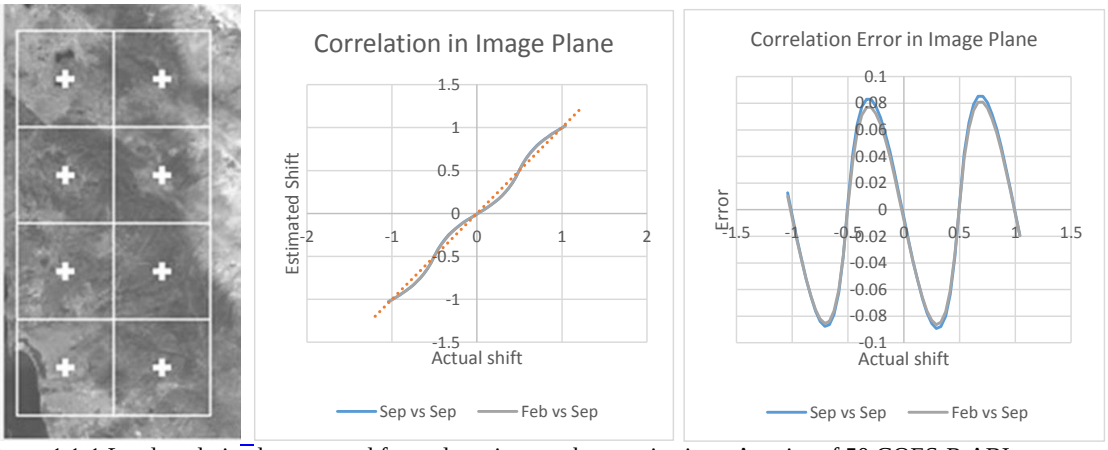

Figure 1.1-1 Landsat-derived scene used for early stair-step characterization. A series of 50 GOES-R ABI surrogate images shifted by 1 Landsat pixel were made by pixel aggregation. The image series sweeps through a two-pixel GOES translation. The center plot shows the estimated image shift, while the right plot is a high-resolution image of the estimation error.

The correlation plot shows characteristics typical of stair-step estimation error. The slope of the estimation curve is lower near the whole-pixel shift points and steeper halfway between these points. The size of the error is also typical. Estimation algorithms with large stair-step error are typically rejected as too inaccurate for subpixel position estimation.

1.2 Mathematical description of the stair-step error

The image registration process can be viewed mathematically as a mapping from an image pair (I_{ref}, I_{test}) and a set of pairs of integer valued translations (m, n) to a matrix of correlation metrics:

Eq. 1.2-1 $$\mathcal{F}\left(I_{ref}, T_{m,n}(I_{test})\right) = C_{m,n}\ ,$$

where $m\ \varepsilon\ \{-M, -M+1, \ldots, 0, \ldots, M-1, M\}$, $n\ \varepsilon\ \{-N, -N+1, \ldots, 0, \ldots, N-1, N\}$, I_{ref} is a reference or "truth" image, I_{test} is a test image, and $T_{m,n}$ is an operator that translates an image m pixels horizontally and n pixels vertically. The reference and test images are assumed to have the same size, P x Q, where P is the number of pixels in the horizontal direction and Q is the number of pixels in the vertical direction. An image translation to the right by 1 pixel is accomplished by the following mapping: $T_{1,0}\left(I_{test,p,q}\right) = I_{test,p+1,q}$. This active shift of pixels within the test image creates vacancies in the entire first column on the left of the test image. The operator $\mathcal{F}$ calculates the correlation metric of its two image-valued arguments within the symmetric overlap region of these images, such that both images are cropped to size (P-m, Q-n) before the correlation metric is calculated. Image registration techniques work well when misregistrations are much smaller than image size, i.e., M << P and N << Q, and we adopt this constraint in what follows. Since the correlation matrix is finite, it will have a global maximum for some pair of shifts (m_{pk},n_{pk}). This maximum may not be unique, but for the moment we assume that it is. Since the reference and shifted test images are most similar for a translation (m_{pk},n_{pk}), we consider the test image to be misregistered with respect to the reference image by m_{pk} pixels horizontally and by n_{pk} pixels vertically.

We are interested in accurately inferring subpixel misregistrations. We apply a method for estimating the location of the "true" peak correlation metric at non-integer values. We determine the unique parabola that passes through the values of the correlation metric at (m_{pk},n_{pk}) and its two nearest neighbors in the horizontal direction, (m_{pk}-1,n_{pk}) and (m_{pk}+1,n_{pk}). The location of the maximum of this parabola, which in general takes non-integer values, represents the peak location refinement in the horizontal direction. We perform a similar operation in the vertical direction to refine the vertical peak location.

For simplicity, we assume that the test image is acquired by an imaging system identical to the system that acquires the reference image, but with an unknown boresight shift (r, s) relative to the boresight of the imaging system that acquires the reference image. The parameter r is an arbitrary shift in the horizontal direction, measured in fractional pixels, and s is a similar arbitrary shift in the vertical direction. The true misregistration of the test image relative to the reference image is defined by the test image boresight shift, and we will use the terms "true misregistration" or "true test image misregistration" interchangeably with "test image boresight shift" in what follows. We further assume that the imaging system point spread function and horizontal and vertical sampling intervals are independent of the scene viewing direction. This uniformity assumption will allow us to establish a relationship between boresight shifts and test image translations that is central to this mathematical description, as will be seen below.

We now rewrite Eq. 1.2-1 for the class of test images we have chosen:

Eq. 1.2-2 $$\mathcal{F}\left(I_{ref}, T_{m,n}\left(I_{test}(r,s)\right)\right) = C_{m,n}(r,s)$$

where $I_{test}(r,s)$ is the image acquired with a boresight shift (r,s), or, equivalently, with true misregistration (r,s), and $C_{m,n}(r,s)$is the (m,n) entry of the correlation matrix of the reference image and the (r,s) misregistered test image. Note that by definition of how the test image is related to the reference image:

Eq. 1.2-3 $$I_{test}(0,0) = I_{ref}$$

and $C_{m,n}(0,0)$ is the autocorrelation function of I_{ref}. We can also define the registration error ϵ_{reg} as an estimated boresight shift (r_{est}, s_{est}) minus the true boresight shift (r,s):

Eq. 1.2-4 $$\varepsilon_{reg} = (r_{est} - r, s_{est} - s)$$

Observe that a translation of the test image with zero boresight shift by (m,n) pixels can be exactly compensated within the cropped sub-image of size (P-m, Q-n) by a boresight shift of the test image by equal and opposite integer numbers of pixels (-m,-n). This is so because a horizontal translation of the test image to the right, as an active translation, shifts image features to the right, whereas a horizontal boresight shift to the right shifts these same features to the left. Similar statement holds for horizontal boresight shift to the left, and vertical boresight shifts either up or down. Therefore, the following relationships hold within the cropped sub-image of size (P-m, Q-n):

Eq. 1.2-5 $$\mathcal{F}\left(I_{ref}, T_{m,n}\left(I_{test}(m',n')\right)\right) = \mathcal{F}\left(I_{ref}, T_{0,0}\left(I_{test}(m'-m,n'-n)\right)\right) = \mathcal{F}\left(I_{ref}, T_{m-m',n-n'}\left(I_{test}(0,0)\right)\right)$$

for $m' \leq m$ and $n' \leq n$.

Or, equivalently in terms of the correlation matrices, the following relationships hold for the cropped sub-image of size (P-m, Q-n):

Eq. 1.2-6 $$C_{m,n}(m',n') = C_{0,0}(m'-m,n'-n) = C_{m-m',n-n'}(0,0)$$

for $m' \leq m$ and $n' \leq n$.

If the restriction to the cropped sub-image of the test image is removed, then the above relationships hold only approximately, but the approximation will be quite good if all shifts are much less than the image size, i.e., $m \ll P,\ m' \ll P,\ n \ll Q,\ n' \ll Q$.

We now present an example that illustrates how the stair-step error arises and its characteristics for two methods for estimating misregistration from the correlation matrix. We consider one-dimensional images for simplicity.

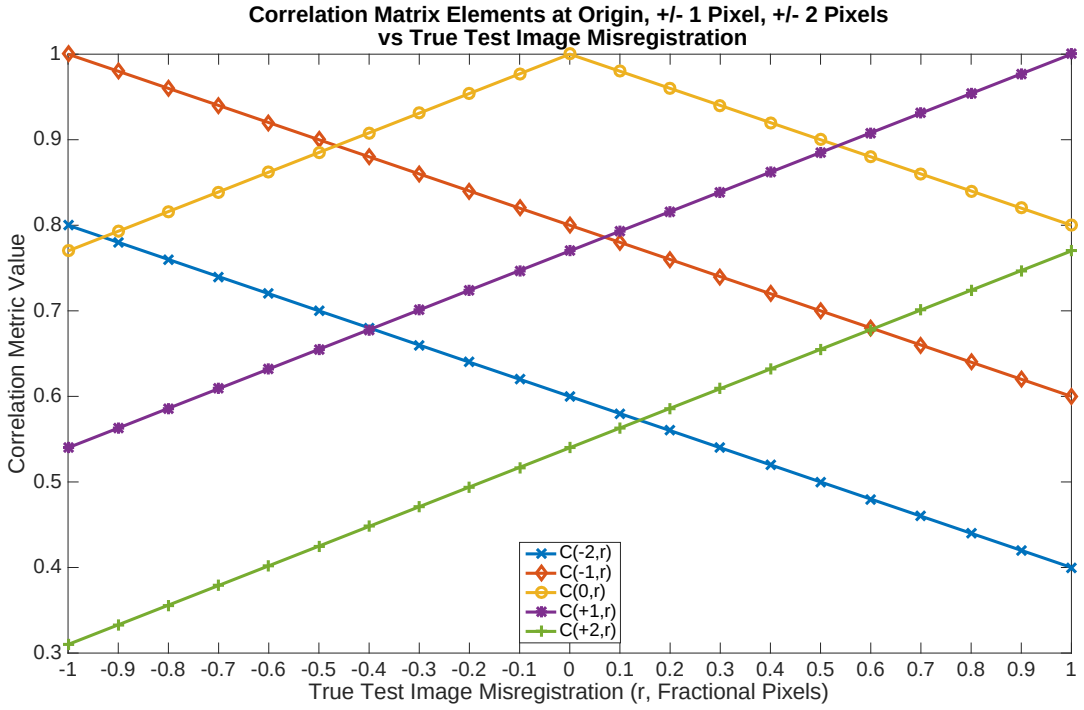

Figure 1.2-1. Correlation metric versus true misregistration error for five adjacent correlation metrics within the correlation matrix.

Figure 1.2-1 shows the correlation metrics for five neighboring members of the correlation matrix, namely $C_{-2}(r)$, $C_{-1}(r), C_0(r), C_{+1}(r), C_{+2}(r)$ as functions of the test image true misregistration for real values r in the range [-1, +1]. Note that the second dimension has been dropped. The correlation metric behavior shown is notional, Note that by Eq. 1.2-2 and Eq. 1.2-3, $C_0(0) = 1$. The notional traces in Figure 1.2-1 have been generated using a linear drop-off for convenience, but the actual behavior will not be linear. Note also that the behavior of the correlation metric as a function of test image translation is not in general left-right symmetric even for zero misregistration error, i.e., $C_m(0) \neq C_{-m}(0)$, for $m \neq 0$, and this asymmetric behavior has important consequences for the behavior of the staircase error. In the example illustrated in Figure 1.2-1 we have chosen $C_{-1}(0) = 0.80$ and $C_{+1}(0) = 0.77$.

The traces in Fig. 1.2-1 for $C_m(r)$, $m \neq 0$, are constructed by translation of the trace for $C_0(r)$ using the relationships in Eq. 1.2-6, extended to non-integer values of the misregistration error r, and assuming our images are large enough so that we can ignore the small errors associated image cropping effects. The relationships in Eq. 1.2-6 provide tie points relating the traces for $C_m(r)$, $m \neq 0$, to the trace for $C_0(r)$ for integer values of true misregistration, as long as these integer values are much smaller than image size. Translation of the trace for $C_0(r)$ as whole, including arbitrary, non-integer true misregistration errors, can be justified by imagining that the integer portion of the misregistration error r is compensated by a shift of the reference image by this integer value. Both the reference and test images after such a shift represent observations of a slightly different, shifted portion of the scene by their respective imaging systems, but otherwise the situation is the same as our starting point in this model. The slight difference in the viewed scene results in small differences in the correlation matrix elements for a given test image boresight shift. However, these differences are of the same order as the cropping effect errors that we are already ignoring. In summary, then, Figure 1-2.1 shows the qualitative behavior that one would find by performing actual calculations using real images and a selected correlation metric, and this qualitative behavior is all that is needed to describe the qualitative behavior of the stair-step error.

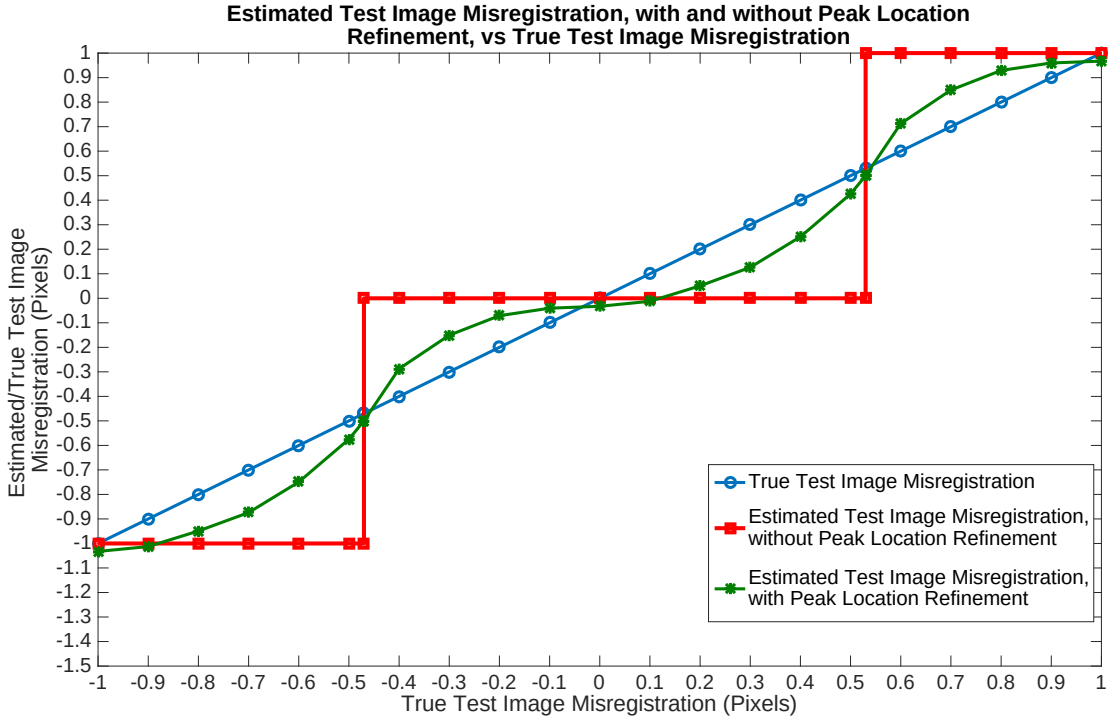

Fig. 1.2-2 Estimated versus true test image misregistration for two choices of the estimation algorithm, one using the location of the peak correlation metric alone, and the other using parabolic peak location refinement. The diagonal showing true misregistration versus true misregistration is also shown for reference.

Figure 1.2-2 maps the correlation metrics displayed in Figure 1.2-1 for true misregistrations r into estimates r_{est} of the true misregistration using the two estimation algorithms already mentioned, the algorithm that chooses the location of the peak correlation metric in the correlation matrix as the estimate, and the algorithm that applies parabolic peak location refinement to the peak correlation metric and its two nearest neighbors. The horizontal axes of these two figures is identical, so the values of the one or three correlation metrics ingested by the misregistration estimation algorithm can be read off from a vertical slice of Figure 1.2-1 at the true misregistration of interest. As mentioned above, the simplest way to estimate the misregistration, at least to the nearest pixel, is to identify the peak correlation metric in the correlation matrix. We can read off from the plot in Fig. 1.2-1 that the peak correlation metric is at the origin within the correlation matrix as long as the test image boresight shift lies in the range (-0.47, +0.53), so that r_{est} =0. For boresight shifts in the range (-1.47, -0.47) the peak correlation metric lies one pixel to the left of the origin, so that r_{est} =-1. For boresight shifts in the range (+0.53, +1.53) the peak correlation metric lies one pixel to the right of the origin, so that r_{est} =+1 . The resulting stair-step pattern is illustrated in Fig. 1.2-2 for the interval [-1, +1]. This pattern illustrates exactly the stair-step artifact defined as a systematic bias of the image registration towards the nearest shift of an integral number of pixels The stair-step error is the difference between the stair-step horizontal line segments representing the estimated test image misregistration and the diagonal representing the true misregistration error and has a triangular or "sawtooth" behavior. The origin of the stair-step error for this simplest estimation algorithm is the finite sampling in the imaging plane, which in turn results in finite sampling in the correlation plane and therefore the inability to resolve sub-pixel misregistrations. As this example illustrates, the locations of the steps need not lie exactly halfway between pixels. The step locations are scene dependent. Note also that the staircase pattern extends in the correlation plane until the overlap region of the image pair being correlated becomes too small for meaningful correlation.

Fig. 1.2-2 also illustrates the behavior of the estimated test image boresight shift when parabolic peak location refinement is applied. The effect of peak location refinement is to smooth the stair-step estimated misregistration into a sinusoid-like, cyclic estimated misregistration. The misregistration error in this case is the difference between the misregistration estimated using parabolic peak location refinement and the diagonal. It can be seen that this error is generally smaller using the improved algorithm.

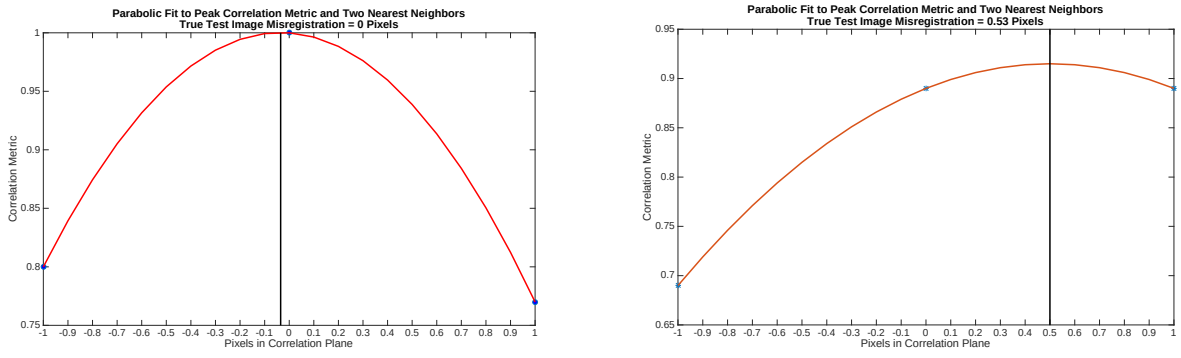

Fig. 1.2-3 The plot on the left illustrates that parabolic peak location refinement in general generates an error at integer values of the true test image misregistration due to the left-right asymmetry of the triple of correlation metric values used in the refinement. The plot on the right illustrates that the refined peak location lies exactly midway between two pixels for which the correlation coefficients are equal.

Parabolic peak location refinement reduces the stair-step error for the single peak algorithm to zero in the neighborhood of the discontinuity in the stair-step error, where the stair-step error is maximum. We give below a heuristic argument for why this must be so. Here we note that at the point of the stair-step discontinuity, two of the three correlation coefficients are both maxima and equal. In this case the parabolic refinement always generates the midpoint of the integer shifts associated with the equal pair of correlation coefficients. This can be seen by considering a parabola with a local maximum midway between the two points at which the correlation coefficients are equal and adjusting the value of the local maximum until the third smaller correlation coefficient lies on the parabola. For the case illustrated in Figure 1.2-1 two of the three correlation coefficients are equal to one another where the trace for $C_0(r)$ intersects the trace for $C_{+1}(r)$ at $r \cong 0.53$ pixels with a value of approximately 0.89. The estimated misregistration is exactly 0.5 at this point, resulting in a very small misregistration error. The misregistration error is exactly zero where the estimated misregistration trace crosses the diagonal just to the right of the stair-step discontinuity on the right in Figure 1.2-2. The parabolic peak location refinement for the case in which the two correlation coefficients are equal at the true test image misregistration of about 0.53 pixels is illustrated in Fig. 1.2-3, along with the case for which the true test image misregistration is zero.

Although the detailed shape of the staircase cycle for parabolic peak location refinement is scene dependent, there are two features of its behavior that always hold true, at least within the domain of small test image translations and boresight shifts relative to image size. One feature is that the cyclic error always has a node, or zero error point, as mentioned above, somewhere between each pair of adjacent integer shifts within the correlation matrix. This is so because the slope of the estimated test image misregistration, as a function of true test image misregistration, is almost exactly the same at integer values of true test image misregistration. If the absolute value of this slope is less than one, as is usually the case, then the estimated test image misregistration undershoots the diagonal shown in Figure 1.2-2 at a pair of successive integer values of the true test image misregistration. By continuity the estimated test image misregistration must cross the diagonal at some point between these two integer valued true test misregistrations. The argument is the same if the magnitude of the slope of the estimated test image misregistration is greater than one at integer values of the true test image misregistration.

The second feature of the cyclic staircase error that holds true in general, again within the domain of small test image translations and boresight shifts relative to image size, is that the shape of staircase error as a function of true boresight shift between adjacent integer shifts is very nearly the same between any two adjacent integer shifts. This feature follows from Eq. 1.2-6 by an argument made above.

We now present an argument to explain why the parabolic peak refinement method generates an estimated image misregistration biased toward the nearest shift of an integral number of pixels. To do so, we must show that the absolute value of the slope of the estimated misregistration dr_{est}/dr is less than one at r = 0. Using the equations that determine the unique parabola that passes through three points, one finds the following formula for the estimated misregistration:

Eq. 1.2-7
$$r_{est} = \frac{C_{+1}(r) - C_{-1}(r)}{4C_0(r) - 2C_{-1}(r) - 2C_{+1}(r)}$$

Taking the derivative with respect to the true misregistration r and evaluating at r = 0, we have:

Eq. 1.2-8
$$\frac{dr_{est}}{dr}(0) = \left[\frac{\frac{dC_{+1}(r)}{dr} - \frac{dC_{-1}(r)}{dr}}{4C_0(r) - 2C_{-1}(r) - 2C_{+1}(r)} - \left(C_{+1}(r) - C_{-1}(r)\right) \frac{4\frac{dC_0(r)}{dr} - 2\frac{dC_{-1}(r)}{dr} - 2\frac{dC_{+1}(r)}{dr}}{\left(4C_0(r) - 2C_{-1}(r) - 2C_{+1}(r)\right)^2} \right]_{r=0}$$

To make further progress we must assume a definite and realistic functional form for $C_0(r)$. We choose an exponential form as follows:

Eq. 1.2-9
$$C_m(r) = e^{-sign(r-m)(r-m)/\mu}$$

where μ is the correlation length, defined as the test image boresight shift at which the correlation between the test and reference images falls to 1/e. The sign(r-m) function appears in the exponent because the correlation can be increasing or decreasing depending upon the values of r and m, as shown in Figure 1.2-1. Substituting the above functional form in Eq. 1.2-9 yields:

Eq. 1.2-10
$$\frac{dr_{est}}{dr}(0) = \left[\frac{\frac{1}{\mu}\left(1 + \frac{r-1}{\mu}\right) + \frac{1}{\mu}\left(1 - \frac{r+1}{\mu}\right)}{4 - 2\left(2 - \left(\frac{2}{\mu}\right) + \left(\frac{1}{\mu}\right)^2\right)} \right]_{r=0} \cong \frac{\frac{2}{\mu}\left(1 - \frac{1}{\mu}\right)}{4 - 2\left(2 - \left(\frac{2}{\mu}\right) + \left(\frac{1}{\mu}\right)^2\right)} \cong \frac{1}{2} \frac{\left(1 - \frac{1}{\mu}\right)}{\left(1 - \frac{1}{2\mu}\right)} \cong \frac{1}{2}\left(1 - \frac{1}{2\mu}\right)$$

where we have expanded in the parameter $1/\mu$, keeping only terms of first order. We know from direct calculation that the correlation length of ABI-like images varies from several pixels to ten or more pixels, so our expansion parameter is

indeed less than one, as it must be, for the images in which we are interested. We have also used the fact that $C_{+1}(0) = C_{-1}(0)$ to eliminate the second term on the right hand side of Eq. 1.2-8. This demonstration that the slope of the estimated misregistration is substantially less than one, in fact less than 0.5, connects the behavior of the stair-step to image correlation length in a manner that makes intuitive sense. The greater the image correlation length relative to one pixel, the less the pixelation of the image should matter.

In order to provide a mathematical description of the stair-step error in this section that is as general as possible, we have not specified the correlation metric, other than to require that the correlation metric drop off as the images being compared become more dissimilar. All of the simulation results shown in this paper use the Pearson correlation coefficient as the correlation metric. This correlation coefficient is defined by mapping the two-dimensional images into one dimensional vectors using a common ordering scheme, subtracting off the mean, and calculating the normalized inner product as follows:

Eq. 1.2-11
$$CC_{Pearson}(I_1, I_2) = \frac{\langle I_1, I_2 \rangle}{\|I_1, I_1\| \|I_2, I_2\|}$$

where I_1 and I_2 are the one-dimensional versions of the two images with mean values subtracted, $\langle \ldots \rangle$ denotes the vector inner product, $\| \ldots \|$ denotes the associated vector norm, and $CC_{Pearson}(I_1, I_2)$ denotes the Pearson correlation coefficient.

1.3 Minimizing stair-step by correlating at higher resolution

The best method we have found to reduce the impact of stair-step error on estimation accuracy is to use high-resolution truth chips. In the case of GOES-R ABI NAV, our truth chips are formed by transforming Landsat images to the viewpoint of the GOES satellite. The truth data has much higher resolution than the GOES imagery. An intermediate resolution level is chosen for correlation. The GOES data is up-sampled to this resolution, and the truth data is down-sampled so that the two images are at a common resolution for correlation.

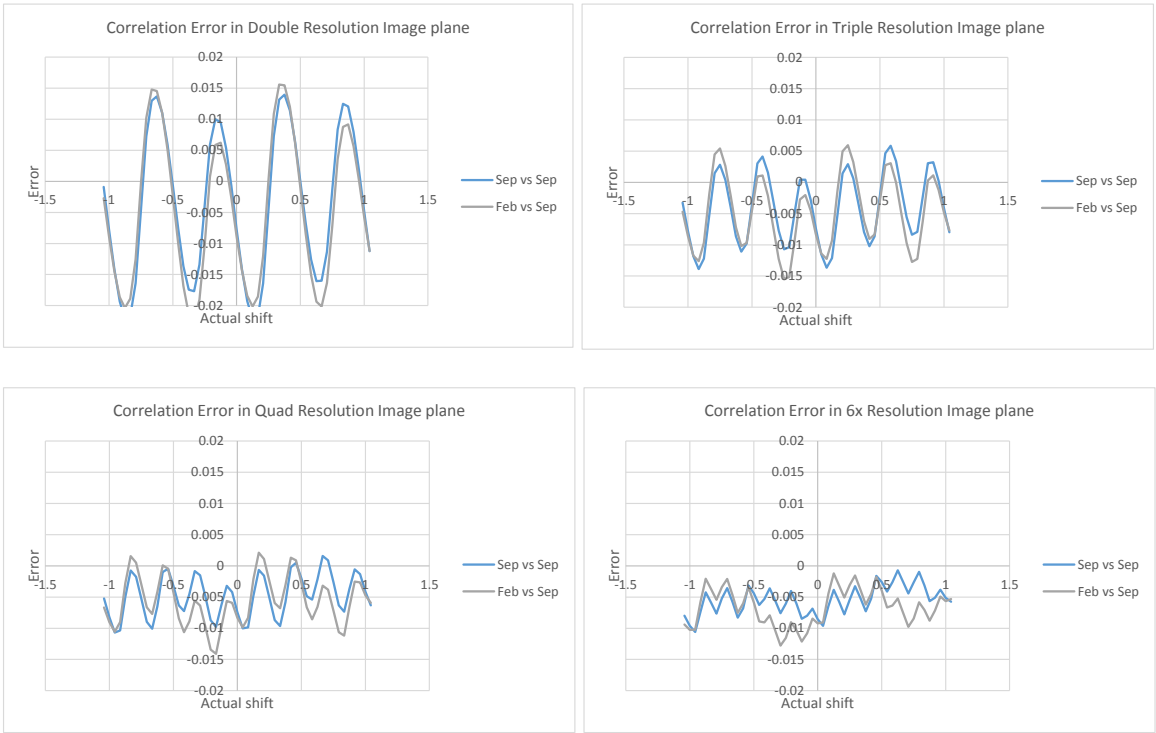

Figure 1.3-1. Correlation error for the scene in Figure 1 when correlation is performed against a high-resolution truth map.

Figure 1.3-1 shows the result of increasing the resolution of the reference windows in the simulation described in Figure 1 by factors of 2, 3, 4, and 6. When the resolution of the truth reference is doubled, the RMS error is reduced from 0.06 pixel RMS to 0.012. The period of the stair-step function has also been cut in half to match the resolution of the higher-resolution truth pixels. The triple, quad, and 6x resolution increases result in RMS errors of 0.007, 0.006, and 0.006 pixels. Continuing improvement is seen, but it does not match the initial improvement. The offset of ~0.005 pixels, which is seen in all of the estimates, plays an increasing role in the RMS value. Making a selection of the "best" approach to minimize this error requires balancing the RMS total error with the needs of the program and the computational overhead of correlating high-resolution images with a corresponding increase in the number of pixels.

Another limitation on this method is that it only works when there is a higher-resolution image to correlate to. For cases like FFR, where the goal is generally correlating to an image of the same native resolution, this approach isn't an option. If both images are up-sampled to reach the correlation resolution, accuracy is not improved. A good subpixel interpolator in the output plane is a better and more efficient option than interpolating the inputs and correlating larger image arrays.

1.4 Estimating the error and subtracting it

Another approach to reducing the impact of a minor stair-step artifact is to estimate the size of the artifact and subtract it. From examining Figures 1.1-1 and 1.3-1, it is apparent that a mild stair-case is roughly sinusoidal in shape, and the error has zeros at the integral and half pixel points. If the magnitude of the stair-step error at ¼ pixel maximum can be estimated this approach works very well. Figure 1.4-1 shows that for the case shown in Figure 1.1-1 (a simple stair-step of 0.08 pixel magnitude), this reduces error from 0.06 RMS to 0.009, performing slightly better than correlating at double resolution.

This performance improvement was a result of a very good estimate for the magnitude of the stair-step artifact. A high-quality quantization of the artifact is not generally available. The stair-step amplitude is image/resolution-dependent and correlator-dependent, but its average amplitude can often be characterized reasonably well. If the amount of stair-step is overestimated, the error is bounded by the case where there is actually no stair-step present, and the entire correction introduces error. If the staircase is underestimated, the estimated correction will compensate part, but not all of the error. The estimate is improved, but by less than the magnitude of the artifact.

For correlators we consider well matched to the data we are correlating, we have seen stair-case amplitude ranging from 0.05 pixel RMS to 0.12 pixel RMS for the quadratic correlation peak interpolation we have described here. For this range, the 0.06 amplitude stair-step assumption would be a reasonable assumption. Before selecting a value it is worthwhile to conduct a study using images typical of those that the correlator will compare to develop a more solid basis for predicting the amplitude of stair-step expected.

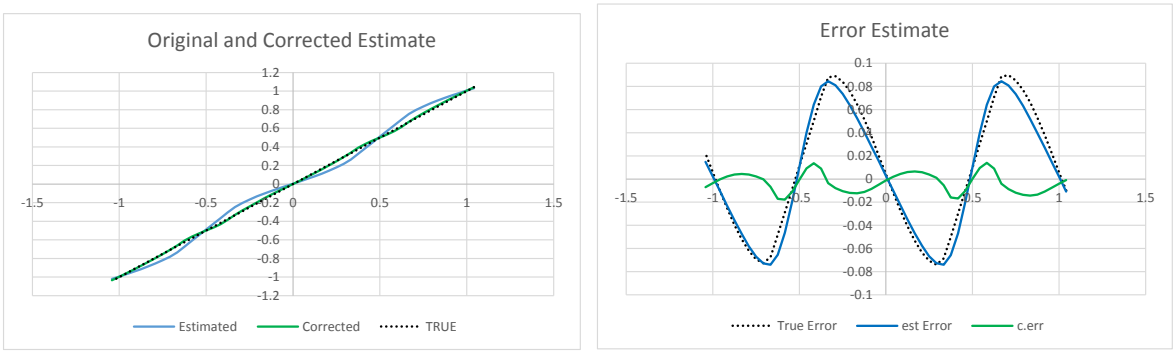

Figure 1.4-1. The resultant error when stair-step in Fig. 1 is estimated as sinusoidal and subtracted is 0.009 pixel RMS.

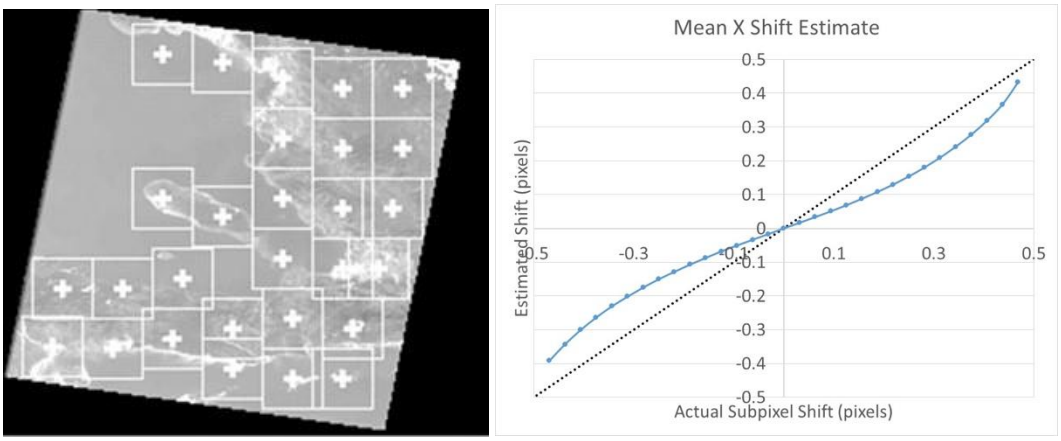

Figure 2.1-1. Landsat-derived scene for testing IPATS. The plot shows average autocorrelation response to an east-west shift.

2. A TEST SCENE RUN IN IPATS

2.1 Autocorrelation stair-step effects in Landsat band 3

Figure 2.1-1 shows a Landsat 7 scene which we have used throughout prototyping of IPATS. Subpixel motion was modeled in both dimensions for just under a full pixel of motion. The illustration here is for east-west shift, with the center-point chosen at the center of the modeled motion. Correlation locations have been hand-selected to minimize overlap and areas which are primarily water, and to avoid having any correlation region cross the boundary of the Landsat chip. The registration regions are 930x930 Landsat pixels, and are aggregated to 30x30 surrogate ABI red band (0.64 μm) pixels.

The RMS error is 0.08 pixels, compared to the 0.06 pixel error in the San Diego Scene. The 28 correlation windows are 30x30, compared to eight 48x48 windows in the San Diego scene. The average shift shows classic staircase behavior. The estimated position crosses the true offset line when there is no shift and at approximately $\pm$ ½ pixel shift. The slope of the estimate line is reduced passing though zero, and is higher than 1 when crossing at half pixel shift. The error is approximately sinusoidal.

3. ESTIMATING FLIGHT STAIR-STEP

The impact of stair-step in operational data can be directly assessed for the NAV case. Since it makes no difference if the motion to be evaluated is motion of the satellite data or motion of the reference data, a reference series can be made containing subpixel motion, and correlation with this set can be used to evaluate stair-step behavior. The navigation references are formed starting with Landsat 8 images. An intermediate step in the current process results in a set of reference chips from the GOES satellite viewpoint at 12 times GOES resolution. For a select locations, a set of reference NAV chips can be made at these subpixel offsets along a straight line path. If these chips are registered with a GOES image, and the registration offsets plotted as they are here, the magnitude of stair-step error in the registration product is determined in the same manner as done here. The estimated motion of the image through the set of references will show motion with stair-step error. The size of the stair-step is estimated from the departure from the straight-line motion imposed on the reference series.

The magnitude of stair-step error cannot be quantified for FFR, SSR, and CCR estimates in this way, since there is no set of higher-resolution reference images. However, it can be estimated based on the response of similar imagery to a quarter-pixel shift. The NAV registration points provide an excellent source of this similar imagery. This may result in an estimate

for stair-step that is not exactly correct for the image being registered, but it has already been pointed out that while this will not result in the best estimate possible, it is generally more accurate than an estimate that does not consider stair-step.

4. CONCLUSIONS

The stair-step artifact has been described, and its impact on GOES-R image characterization using IPATS has been evaluated. Errors of 0.06 and 0.08 pixel RMS have been demonstrated for well-behaved, single waveband data. A mathematical description has been presented that shows the origin of a pure stair-step for the simplest image misregistration algorithm and the milder stair-step that results from using a peak location refinement algorithm in the correlation plane. The approximately periodic nature of the stair-step artifact and the existence of zeroes in the stair-step error occurring about halfway between integer misregistrations have been demonstrated. For the parabolic peak location refinement method used by IPATS and a realistic choice of the image correlation functional form, the stair-step behavior has been shown to be connected to the magnitude of the image correlation length in a way that makes sense.

A method has been described for estimating the magnitude of this artifact in operational data. Two methods have been described for compensating this effect by adding a correction to the correlation output. The more capable method uses increased resolution registration, and requires that the reference image be available at a higher resolution than the image whose location is to be determined by registration. This method will work well for NAV processing. The less robust method requires an approximation of the magnitude of the stair-step artifact, and can be obtained through NAV analysis of similar imagery. This approximate stair-step is subtracted from the registration estimate. An example was shown where this method reduced stair-step error from 0.06 to 0.009 pixels RMS.

REFERENCES

[1] Grycewicz, T. J., Florio, C. J., Franz, G. A., Robinson, R. E., "Estimation bias from using nonlinear Fourier plane correlators for sub-pixel image shift measurement and implications for the binary joint transform correlator," Proc. SPIE 6695, 66950J (2007).

[2] De Luccia, F. J., Houchin, S., Porter, B. C., Graybill, J., Haas, E., Johnson, P. D. Isaacson, P. J., Reth, A. D., "Image navigation and registration performance assessment tool set for the GOES-R Advanced Baseline Imager and Geostationary Lightning Mapper," Proc. SPIE 9881, 988119 (2016).

[3] Carr, J. L., J. Fox-Rabinovitz, D. Herndon, S. Reehl, "Verifying the Accuracy of Geostationary Weather Satellite Image Navigation and Registration", Ninth Annual Conference on Future Operational Environmental Satellite Systems, 93rd American Meteorological Society Meeting (2013).

[4] GOES-R Series Mission Requirements Document (MRD), GOES-R-Program/Code 410, 410-R-MRD-0070, Version 3.20, January 2016, http://www.goes-r.gov/syseng/docs/MRD.pdf

[5] Pearson, K., "Notes on regression and inheritance in the case of two parents," Proc. Royal Society London 58, 240-242 (1895).

[6] Wikipedia contributors, "Pearson product-moment correlation coefficient," Wikipedia, The Free Encyclopedia, 28 May 2016, https://en.wikipedia.org/wiki/Pearson_product-moment_correlation_coefficient (30 June 2016).

[7] OpenCV v. 3.1, 21 Dec 2015, http://opencv.org/ (30 June 2016).

[8] Landsat images LC80400372013110LGN01 and LC80400372014273LGN00.